RESEARCH ARTICLE | MARCH 15 2021

Anisotropic thermal conductivity measurement of organic thin film with bidirectional 3ω method

Shingi Yamaguchi ; Takuma Shiga ; Shun Ishioka; Tsuguyuki Saito ; Takashi Kodama ; Junichiro Shiomi

Rev. Sci. Instrum. 92, 034902 (2021)
https://doi.org/10.1063/5.0030982

Review of Scientific Instruments ARTICLE scitation.org/journal/rsi

Anisotropic thermal conductivity measurement of organic thin film with bidirectional 3ω method

Cite as: Rev. Sci. Instrum. 92, 034902 (2021); doi: 10.1063/5.0030982
Submitted: 26 September 2020 • Accepted: 24 February 2021 •
Published Online: 15 March 2021

Shingi Yamaguchi,[1] Takuma Shiga,[1] Shun Ishioka,[2] Tsuguyuki Saito,[2] Takashi Kodama,[1] and Junichiro Shiomi[1,a)]

AFFILIATIONS

[1] Department of Mechanical Engineering, The University of Tokyo, 7-3-1, Hongo, Bunkyo-ku, Tokyo 113-8656, Japan
[2] Department of Biomaterial Sciences, Graduate School of Agricultural and Life Sciences, The University of Tokyo, 1-1-1 Yayoi, Bunkyo-ku, Tokyo 113-8657, Japan

[a)] **Author to whom correspondence should be addressed:** shiomi@photon.t.u-tokyo.ac.jp

ABSTRACT

Organic thin film materials with molecular ordering are gaining attention as they exhibit semiconductor characteristics. When using them for electronics, the thermal management becomes important, where heat dissipation is directional owing to the anisotropic thermal conductivity arising from the molecular ordering. However, it is difficult to evaluate the anisotropy by simultaneously measuring in-plane and cross-plane thermal conductivities of the film on a substrate because the film is typically as thin as tens to hundreds of nanometers and its in-plane thermal conductivity is low. Here, we develop a novel bidirectional 3ω system that measures the anisotropic thermal conductivity of thin films by patterning two metal wires with different widths and preparing the films on top and extracting the in-plane and cross-plane thermal conductivities using the difference in their sensitivities to the metal-wire width. Using the developed system, the thermal conductivity of spin-coated poly(3,4-ethylenedioxythiophene) polystyrene sulfonate (PEDOT:PSS) with thickness of 70 nm was successfully measured. The measured in-plane thermal conductivity of PEDOT:PSS film was as high as 2.9 W m^{-1} K^{-1} presumably due to the high structural ordering, giving an anisotropy of 10. The calculations of measurement sensitivity to the film thickness and thermal conductivities suggest that the device can be applied to much thinner films by utilizing metal wires with a smaller width.

INTRODUCTION

In the field of electronics, organic thin films are gaining attention because of their semiconductor features.[1,2] Thermal management of these materials is an important issue as heat is generated due to self-Joule heating, and therefore, the evaluation of their thermal conductivity (κ) is essential. Many of these materials take a highly ordered structure in the form of thin film with a thickness less than 100 nm,[3,4] and this structural anisotropy and small thickness have to be considered in the κ measurements. Among the developed measurement techniques for in-plane thermal conductivity ($\kappa_\parallel$) such as the offset time domain thermoreflectance (TDTR) method,[5–7] suspended microdevice,[8,9] and offset laser flash method,[10] the 3ω method[11–16] has the advantage of measuring such thin samples. The 3ω method separately measures cross-plane thermal conductivity ($\kappa_\perp$) and thermal anisotropy ($\eta = \kappa_\parallel/\kappa_\perp$) by detecting the voltage oscillation signal with various widths of metal wires deposited on the sample. The measurement is made sensitive to η by making the width of a narrowest wire as small as the thickness of the thin film. Such metal wires are usually prepared on the target sample by lithography techniques, which can damage organic materials with harsh chemicals in the developing or etching process. Some alternative methods have been proposed for the $\kappa_\parallel$ measurement of organic thin films by fabricating metal wires with shadow mask[17,18] or applying 3ω measurement to a film on a suspended membrane with metal wires.[19,20] However, these methods also have limits on the appreciable sample range; the shadow mask cannot prepare nanometers-wide wire required for the measurement of the submicron-thin film, and the suspended membrane can be destructed by the common spin coating process used for film preparation. Therefore, a general method with wider applicability is required to measure η of organic thin films.

There also exists the bidirectional 3ω method where a sample is placed on metal wires, which is prepared beforehand on a substrate.[21–24] Here, "bidirectional" is named after the directions of heat conduction, in comparison to the conventional 3ω method where the heat conducts unidirectionally [Figs. 1(a) and 1(b)]. While this method can avoid damaging the sample by chemicals, only a single narrow wire has been used to extract $\kappa_\perp$ and η, since the measurement with a wider wire would be insensitive to both $\kappa_\perp$ and η.[25] In this work, we develop a bidirectional 3ω system with wide and narrow wires to measure the anisotropic thermal conductivities of organic thin films. In analogy to the conventional 3ω system [Fig. 1(a)], $\kappa_\perp$was obtained first from the measurement with the wide wire, where thermally conductive Al layer was deposited to selectively suppress the sensitivity to η [Fig. 1(b)], and then, η was obtained from the measurement with the narrow wire without the Al layer. By preparing the wires with different widths on one substrate, the two parameters ($\kappa_\perp$and η) can be obtained from the same sample. The method can measure the thermal anisotropy of the thin organic film with a thickness of less than 100 nm, and the results clarify that $\kappa_\parallel$ of highly ordered organic thin film can be more than three times larger than that ever reported.

EXPERIMENTAL METHOD

Device and sample preparation

The measurement device was designed to have eight metal wires of Ti/Pt with different widths [Fig. 1(c)]. The wire width and the lengths between current probes and between voltage probes [lengths A and B in Fig. 1(d), respectively] are summarized in Table I. Thirty devices were fabricated on the 4-in. quartz wafer at once, and all the processes were conducted in the Takeda cleanroom at the University of Tokyo. Quartz was chosen as the substrate material to suppress heat conduction to the substrate. Ti/Pt (5-nm and 20-nm-thick, respectively) was sputtered on the substrate first, and negative resist for electron beam lithography was spin-coated. The patterns were prepared by direct exposure, development, and subsequent dry etching. A 100 nm alumina (Al_2O_3) layer was deposited on the device as an insulation layer by atomic layer deposition (ALD), while Al_2O_3 on contact pads was removed by the wet-etching process using the photoresist and mask aligner. The wafer was cut into square-shaped devices with the size of 1 cm^2. As the wire with 100-nm width did not survive the dry etching process, the 300-nm-wide wire was used as the narrowest one in this study. Polymethyl methacrylate (PMMA) and PEDOT:PSS films were prepared by spin coating, and part of the film on the contact pads was wiped off before the measurement. The details of sample preparation are provided in the supplementary material.

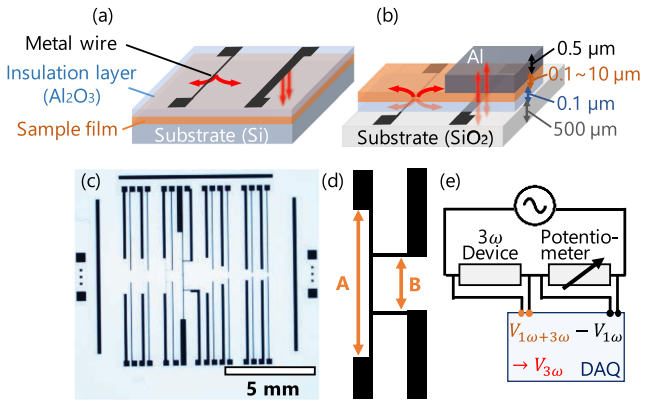

FIG. 1. Schematic image of (a) the conventional 3ω method and (b) bidirectional 3ω method in this work. (c) Picture of the measurement device. (d) Enlarged image of the metal wire. (e) Schematic image of the measurement setup.

TABLE I. Length between the current and voltage probes for each wire width.

Wire width (μm)	50	20	10	2	1	0.5	0.3
Length A (μm)	4500	1800	1800	1800	1800	900	540
Length B (μm)	1500	600	600	600	600	300	180

Solution to the bidirectional heat diffusion equation

The two-dimensional equation of Feldman's algorithm[26] was chosen to take the thermal anisotropy into account. The calculated temperature rise (ΔT) at the wire can be written as

$$\Delta T = \frac{P}{2\pi l}\int_0^\infty \frac{(A^+ + A^-)(B^+ + B^-)}{A^+B^- - A^-B^+}\frac{1}{\gamma_j}\frac{\sin^2(kb)}{(kb)^2}\,dk, \quad (1)$$

$$\gamma_j = \kappa_{j,z}\sqrt{\eta_j k^2 + \frac{2i\omega}{D_{j,z}}}, \quad (2)$$

where P, l, and b are the heating power, length, and half width of the wire, respectively. $\kappa_{j,z}$ and $D_{j,z}$ are the thermal conductivity and thermal diffusivity of the j-th layer in the z direction, and η_j is anisotropy ($\kappa_{j,x}/\kappa_{j,z}$). k is a variable of integration, and A^+, A^-, B^+, and B^- are dimensionless parameters obtained by solving the equation by a recursive matrix method. The details of the mathematical solution and material parameters required for calculation (specific heat capacity and mass density) are included in the supplementary material.

The absolute value of measurement sensitivities ($|S_\beta|$) to the parameters of interest (β) can be calculated using Eq. (1) as

$$|S_\beta| = \left|\left(\frac{\Delta\beta}{\beta}\right)^{-1}\frac{\Delta T(\beta+\Delta\beta) - \Delta T(\beta)}{\Delta T(\beta)}\right|, \quad (3)$$

where $\Delta\beta/\beta$ was set to be 0.1 referring to the previous work.[21]

Measurement setup and analysis procedure

For the measurement, the metal wire on the 3ω device was connected in series with a potentiometer. A schematic of the setup is shown in Fig. 1(e). The potentiometer is adjusted to have the same electrical resistance with that of the wire (R). The temperature coefficient of the resistance (α) of the wire was obtained in advance by measuring the R from 20 °C to 40 °C with the increment of 5 °C. All the measurements were conducted at room temperature (25 °C). Wave current with a frequency ω (10–1500 Hz) was applied, and

the third harmonic voltage across the wire ($V_{3\omega}$) was obtained by subtracting the first harmonic voltage across the potentiometer ($V_{1\omega}$) from that across the device ($V_{1\omega+3\omega}$). The voltage was measured by using DAQ NI-9239 (National Instruments). The temperature rise (ΔT) at the wire was calculated by

$$\Delta T = \frac{2}{\alpha}\frac{V_{3\omega}}{V_{1\omega}}, \tag{4}$$

and the current amplitude ($I_{1\omega}$) was controlled so that the highest ΔT is around 2 K. The target parameters were obtained by fitting the theoretical ΔT [Eq. (1)] with the experimental ones [Eq. (4)] with a least squares method.

The measurement was first conducted with bare device, and the κ of insulation layer (Al_2O_3) was determined for differential measurement. Next, measurements with (i) the film and (ii) the film with Al deposited on the top were conducted to get ΔT. Finally, $\kappa_\perp$ and η of the film were determined in order by fitting the data of (ii) and (i), respectively.

Sources of error

In this study, measurements on a target material were conducted three times with different substrates, and a standard deviation of the obtained values is denoted as the error. Possible sources of the deviation are (1) the fluctuation of the measured signal and (2) the geometric uncertainty of the measurement setup. As for (1), in our system, DAQ functioning as a lock in amplifier can detect the $V_{3\omega}$ signal with a fluctuation as low as 0.2%, which is negligible. Regarding (2), the uncertainties of the wire width and the layer thickness influence the fitting results. As will be discussed later, differential measurements were conducted when obtaining η to eliminate the uncertainty of Al_2O_3 layer thickness, but those of the wire width and the sample thickness remain. Their impact on the target properties can be estimated by inputting the geometries altered by 5% into the physical model to simulate the signal and then fitting it with the physical model, assuming unaltered geometries. For example, with the PMMA film case, the deviation was estimated to be 8% in the cross-plane thermal conductivity and 29% in the thermal anisotropy, which reasonably match with the above standard deviation obtained from multiple experiments.

RESULTS AND DISCUSSION

Before measuring the organic thin films, the thermal conductivity of the 100-nm-thick insulation layer $\kappa_{Al_2O_3}$ was determined. Figure 2(a) shows the measurement sensitivities to $\kappa_{Al_2O_3}$ with wide (50 μm) and narrow (300 nm) wires, which were calculated assuming that $\kappa_{Al_2O_3}$ is the reported value[27] of 2 W m^{-1} K^{-1} and thermal anisotropy $\eta_{Al_2O_3}$ is one. Sensitivities to κ_{SiO_2} were also shown as a reference. While the 50-μm-wide wire has sensitivity only to κ_{SiO_2} and not to $\kappa_{Al_2O_3}$ in the whole frequency range, the 300-nm-wide wire gives the sensitivity to $\kappa_{Al_2O_3}$ as high as 0.2. Therefore, the 300-nm-wide wire was used for the measurement of $\kappa_{Al_2O_3}$. The reason for this sensitivity difference with wide- and narrow-wires is discussed in the supplementary material. As input parameters, measured values were used for thickness and specific heat capacity, while reference values were used for density. The actual values of the parameters are summarized in Table S1. The theoretical curve calculated by Eq. (1) was fitted with the experimental values with a least squares method by altering $\kappa_{Al_2O_3}$ as a fitting parameter. Figure 2(b) shows the experimental temperature rise and best fitted curve for the 300-nm-wide wire. The theoretical curve shows good agreement with the experimental data, and the fitting gives $\kappa_{Al_2O_3}$ of 1.50 ± 0.72 W m^{-1} K^{-1} (N = 6), which is consistent with the reported value.[27] The relatively large error may be due to the uncertainty in the device configuration, such as the wire width and Al_2O_3 thickness, which deviate depending on the device position on the wafer. This uncertainty is eliminated in the measurement of the organic films by the differential technique as described later.

Next, anisotropic κ of the cellulose nanofiber (CNF) oriented film was measured to validate the system. The oriented CNF film was selected as a model sample because its anisotropic κ has been already reported,[28] and in addition, it can be formed either into a film on a substrate or into a self-standing film, which makes it a suitable sample for validation that can be measured by both bidirectional 3ω method and other existing methods. The CNF film thickness measured by using the micrometer was 26 μm. To calculate the measurement sensitivities, reported values of CNF cross-plane thermal conductivity ($\kappa_{CNF,\perp}$) and its thermal anisotropy (η_{CNF}) were used.[28] For thermal boundary resistance (TBR) values at all organic/inorganic interfaces, a reported value of 3 × 10^{-8} m^2 K W^{-1} for the interface

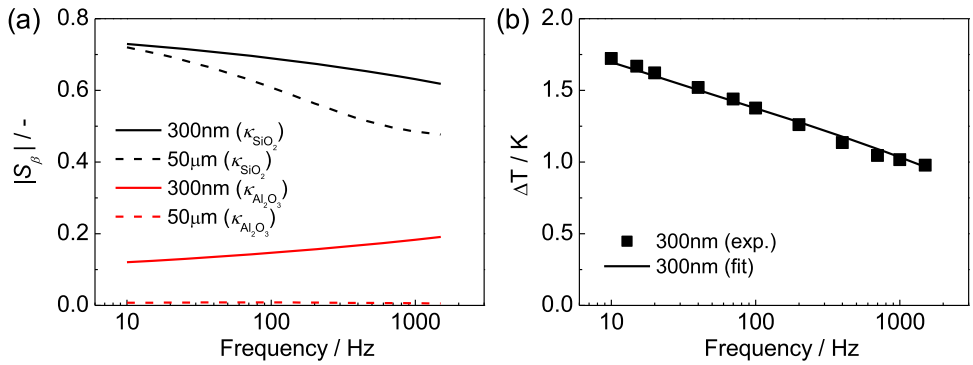

FIG. 2. (a) Sensitivities to $\kappa_{Al_2O_3}$ and κ_{SiO_2} when 300-nm- and 50-μm-wide wires are used. (b) Temperature rise and the fitting curve for the measurement of $\kappa_{Al_2O_3}$ with the 300-nm-wide wire.

between silicon (Si) and spin-coated organic polymer measured by the TDTR method[29] was employed. The absolute value of TBR is not likely to affect the results, as the measurement sensitivity to TBR is less than 0.003 (ee Fig. S1). Sensitivities to $\kappa_{CNF,\perp}$ and η_{CNF} with the 300-nm-wide wires are shown in Fig. 3(a). The sensitivities to $\kappa_{CNF,\perp}$ and η_{CNF} are as high as 0.1–0.2, and another independent measurement is required to suppress uncertainty by determining either one of the parameters.

In conventional 3ω measurement, the films are sandwiched by a metal wire and heat conducting substrate such as Si and the generated heat passes through the film to the substrate [Fig. 1(a)]. In analogy to the conventional system, 500 nm of heat conducting aluminum (Al) was deposited on the CNF film with resistive thermal evaporation so that the heat can conduct in the vertical direction [Fig. 1(b)]. The temperature rise of the sample during deposition is less than several tens of degrees as the melting point of Al is low[30] and the heating effect to the sample is negligible. Al was also deposited on a bare device simultaneously to measure κ of Al (κ_{Al}) in advance (the representative temperature rise and its fitting curve to extract κ_{Al} is shown in Fig. S2). Figure 3(b) shows sensitivity to each parameter when the 50-μm-wide wire is used to measure CNF with the Al deposition. In contrast to the previous 300-nm case, the sensitivity to η_{CNF} is less than 25% of that to $\kappa_{CNF,\perp}$, which means that the measurement is far sensitive to $\kappa_{CNF,\perp}$. Therefore, $\kappa_{CNF,\perp}$ was first determined with the 50-μm-wide wire with the Al deposition, and then, η_{CNF} was determined with the 300-nm-wide wire without the Al deposition. To get those parameters from an identical sample, the measurements of the temperature rises were conducted in reverse order: first without Al case and second with Al case.

$\kappa_{CNF,\perp}$ and η_{CNF} were obtained by the process described above. In addition to the thickness, specific heat capacity, and density (actual values summarized in Table S1), the reference values[28] of $\kappa_{CNF,\perp}$ and η_{CNF} were used as initial input parameters, while the measured value of $\kappa_{CNF,\perp}$ was used when obtaining η_{CNF}. A least squares method was used for fitting by altering $\kappa_{CNF,\perp}$ or η_{CNF} as a fitting parameter in each case. Figures 3(c) and 3(d) show the measured temperature rise and its fitting curve of each case for CNF measurement. $\kappa_{CNF,\perp}$ was determined to be 0.28 ± 0.02 W m^{-1} K^{-1} (N = 3) from the measurement with the 50-μm-wide wire [Fig. 3(d)]. A differential technique was used for the measurement of η_{CNF}; $\kappa_{Al_2O_3}$ was measured beforehand and the value was used in the measurement of η_{CNF}. This method can eliminate the uncertainty resulting from the device configuration as it is included in $\kappa_{Al_2O_3}$. Figure 3(c) shows the temperature rise of the wire with and without CNF, where the difference results from the increased heat conduction to CNF. The measured η_{CNF} was 3.46 ± 0.15 (N = 3), and correspondingly, the $\kappa_{\parallel}$ of CNF ($\kappa_{CNF,\parallel}$) was 0.95 ± 0.04 W m^{-1} K^{-1}. To validate these values, $\kappa_{CNF,\perp}$ and $\kappa_{CNF,\parallel}$ of the self-standing CNF film were also measured by laser flash analysis (LFA)[31,32] and T-type method,[33–35] respectively. The details of each method are described in the supplementary material. $\kappa_{CNF,\perp}$ obtained from LFA was 0.30 ± 0.03 W m^{-1} K^{-1}, and $\kappa_{CNF,\parallel}$ obtained from T-type method was

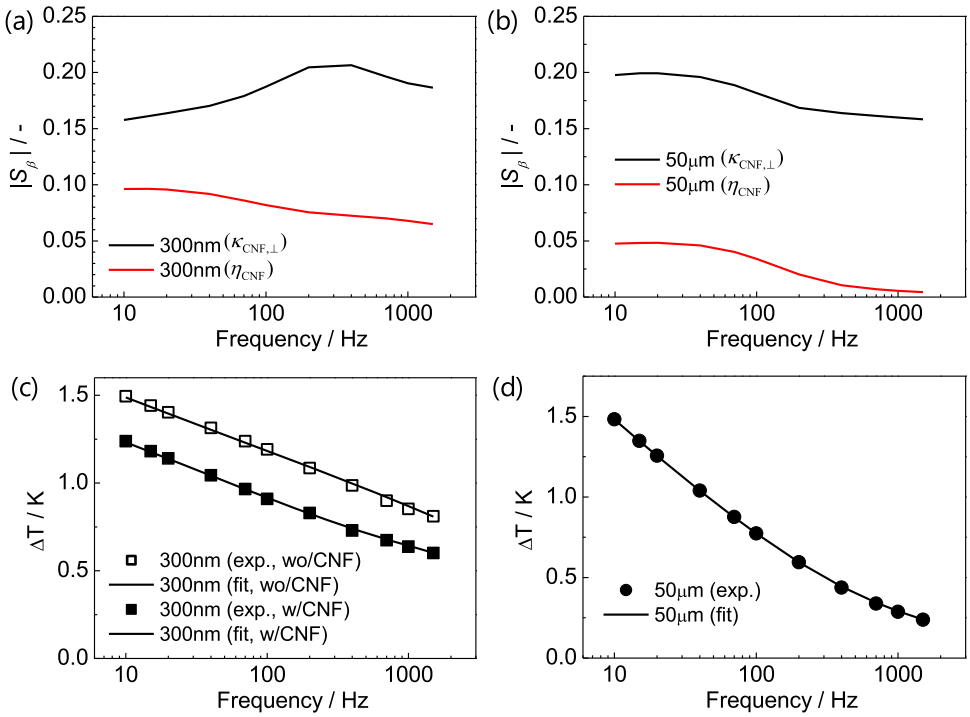

FIG. 3. Sensitivities to $\kappa_{CNF,\perp}$ and η_{CNF} when (a) the 300-nm-wide wire is used without Al deposition and (b) the 50-μm-wide wire is used with Al deposition. Representative temperature rise and its fitting curve for the measurement of $\kappa_{CNF,\perp}$ and η_{CNF} with (c) the 300-nm-wide wire and (d) the 50-μm-wide wire. Control measurement without CNF is also shown in (c).

1.09 ± 0.07 W m^{-1} K^{-1}. These values agree well with the ones obtained from the bidirectional 3ω method, which proves the reliability of this novel method.

Thermal conductivities of spin-casted polymer films were also measured to reveal the anisotropic thermal properties of submicron-thin films. PMMA and PEDOT:PSS were selected as representative materials, and their films were spin-coated on the measurement device. The thicknesses of PMMA and PEDOT:PSS films were 308 nm and 70 nm (measured by interferometry and AFM, respectively). Figure S3 shows measurement sensitivities calculated with the reported cross-plane thermal conductivity and thermal anisotropy of PMMA[17] and PEDOT:PSS.[36] Same as in the CNF case, the sensitivities to both $\kappa_\perp$ and η are large when the narrow wire was used, whereas sensitivities to η are negligible when a wide wire is used with Al deposition. Therefore, the same process was conducted to obtain $\kappa_\perp$ and η of each material (input parameters summarized in Table S1). The measured temperature rise and fitting curves are shown in Fig. S4, and obtained $\kappa_\perp$, η, and $\kappa_\parallel$ are shown in Table II together with the reference values. While $\kappa_\perp$ of PMMA and PEDOT:PSS are close to the reported ones, their $\kappa_\parallel$ are much different from the reference values. The lower value of the measured $\kappa_\parallel$ of PMMA could be due to the difference in the degree of polymer alignment. The PMMA film in this study has a larger thickness (308 nm) than the reported one (170 nm), presumably because of the lower rotation speed in the spin-coat process, which might have led to the lower degree of alignment and hence the lower thermal conductivity.[37,38] On the other hand, $\kappa_\parallel$ of PEDOT:PSS is three to ten times higher than the reported values obtained from thicker films. This can also be explained by the difference of molecular ordering as the thicker films were formed by drop-casting or repeated spin-coatings, and therefore, the 70-nm-thin PEDOT:PSS film is suggested to have high $\kappa_\parallel$ because of its highly ordered structure.

To examine the range of the sample properties and geometries that the current method is applicable to, sensitivities to $\kappa_\perp$ and $\kappa_\parallel$ of model sample with various thicknesses (d) were calculated. The density and specific heat capacity of the model sample were set to 1000 J/kg·K and 1000 kg/m^3, respectively, as representative values of organic materials. The sensitivity of 0.02 was taken as lower bound, considering that $\kappa_{\mathrm{PEDOT:PSS},\parallel}$ can be determined with 30% uncertainty when the sensitivity is 0.02 (Fig. S4). First, the sensitivity to $\kappa_\perp$ of model sample was calculated when the 50-μm-wide wire was used with 1000 Hz alternating current and 500-nm-thick Al is deposited on the sample. An isotropic model sample was assumed in this analysis to show the lowest bound, while the actual sample is expected to have thermal anisotropy. The contour of 0.02 in Fig. 4(a) indicates the lower bound of the measurement, which corresponds to a thermal resistance ($=d/\kappa_\perp$) of ~10^{-7} m^2 K W^{-1}. The measurable smallest film thickness increases from 20 nm to 800 nm as $\kappa_\perp$ increases from 0.1 W m^{-1} K^{-1} to 10 W m^{-1} K^{-1}. This lower bound of thickness can become high if the sample has a thermal anisotropy. Next, the sensitivity to $\kappa_\parallel$ of a model sample was estimated when the 300-nm-wide wire was used with 1000 Hz alternating current without Al deposition. Here, $\kappa_\perp$ of the sample is assumed to be 0.1 W m^{-1} K^{-1}, and the thermal anisotropy was changed from 1 to 100. The contour of 0.02 in Fig. 4(b) indicates the lower bound of the measurement, which corresponds to a thermal conductance ($=d \times \kappa_\parallel$) of ~$10^{-7}$ W m^{-2} K^{-1}. The measurable lowest $\kappa_\parallel$ increases from 0.2 W m^{-1} K^{-1} to 6 W m^{-1} K^{-1} as the film thickness decreases from 1 μm to 10 nm. These bounds can be broadened when a wire with narrower width such as 50 nm is used.

TABLE II. Anisotropic thermal properties of spin-casted polymer films (N = 3).

		$\kappa_\perp$ (W m^{-1} K^{-1})	$\kappa_\parallel$ (W m^{-1} K^{-1})	$\eta(=\kappa_\parallel/\kappa_\perp)$
PMMA	This study	0.22 ± 0.01	0.72 ± 0.18	3.25 ± 0.83
	Reference	0.20–0.25 [17,29,39–41]	2.33 ± 1.55 [17]	...
PEDOT:PSS	This study	0.29 ± 0.11	2.94 ± 0.81	10.1 ± 2.8
	Reference	0.2–0.3 [36,42,43]	0.3–0.8 [20,36,42,43]	...

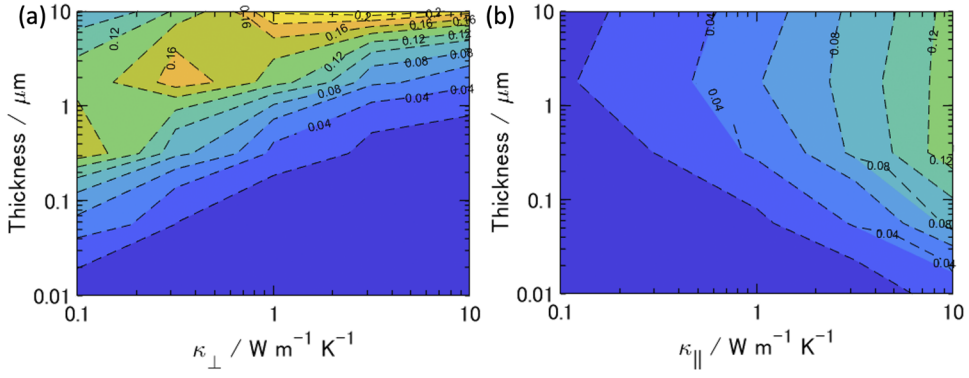

FIG. 4. Contour of the measurement sensitivity to (a) $\kappa_\perp$ and (b) $\kappa_\parallel$ of the model film sample with various thicknesses and κ.

CONCLUSION

A novel bidirectional 3ω system with two different width wires to measure the anisotropic thermal conductivity of an organic thin film was developed. The metal wires of Ti/Pt with widths of 300 nm and 50 μm are patterned on a quartz substrate beforehand, and CNF, PMMA, and PEDOT:PSS thin films were prepared on the substrate. Cross-plane and in-plane thermal conductivity were measured in the sample with the 50-μm- and the 300-nm-wide wires, and this selective measurement was enabled by placing an aluminum layer on the samples in the measurement of cross-plane thermal conductivity and by suppressing the sensitivity to in-plane thermal conductivity. The in-plane thermal conductivity of 70-nm-thick film was successfully measured, revealing that high molecular ordering in the film can increase the in-plane thermal conductivity of the thin film. Sensitivity calculations for various samples with different thermal conductivities and thicknesses clarified the applicable ranges, which suggest the possibility for further improvement by narrowing the wire width.

SUPPLEMENTARY MATERIAL

See the supplementary material for additional information regarding the film preparation, schematic image and solution to the bidirectional heat transfer equation, material parameters, and signal with a fitting curve for 3ω measurement.

ACKNOWLEDGMENTS

This work was supported, in part, by JSPS KAKENHI (Grant Nos. JP18J21726 and 19H00744) and JST CREST (Grant Nos. JPMJCR20Q3 and JPMJCR19I2). This work was conducted at the Takeda Sentanchi Supercleanroom, the University of Tokyo, supported by the "Nanotechnology Platform Program" of the Ministry of Education, Culture, Sports, Science and Technology (MEXT), Japan (Grant No. JPMXP09F20UT0043).

DATA AVAILABILITY

The data that support the findings of this study are available from the corresponding author upon reasonable request.

REFERENCES

[1] C. Wang, H. Dong, L. Jiang, and W. Hu, Chem. Soc. Rev. **47**, 422 (2018).
[2] H. Jiang and W. Hu, Angew. Chem., Int. Ed. **59**, 1408 (2020).
[3] Y. Zhang, J. Qiao, S. Gao, F. Hu, D. He, B. Wu, Z. Yang, B. Xu, Y. Li, Y. Shi, W. Ji, P. Wang, X. Wang, M. Xiao, H. Xu, J. B. Xu, and X. Wang, Phys. Rev. Lett. **116**, 016602 (2016).
[4] A. Yamamura, S. Watanabe, M. Uno, M. Mitani, C. Mitsui, J. Tsurumi, N. Isahaya, Y. Kanaoka, T. Okamoto, and J. Takeya, Sci. Adv. **4**, eaao5758 (2018).
[5] P. Jiang, X. Qian, and R. Yang, Rev. Sci. Instrum. **88**, 074901 (2017).
[6] A. J. Schmidt, X. Chen, and G. Chen, Rev. Sci. Instrum. **79**, 114902 (2008).
[7] J. P. Feser and D. G. Cahill, Rev. Sci. Instrum. **83**, 104901 (2012).
[8] I. Jo, M. T. Pettes, J. Kim, K. Watanabe, T. Taniguchi, Z. Yao, and L. Shi, Nano Lett. **13**, 550 (2013).
[9] A. Weathers, Z. U. Khan, R. Brooke, D. Evans, M. T. Pettes, J. W. Andreasen, X. Crispin, and L. Shi, Adv. Mater. **27**, 2101 (2015).
[10] P. Goli, H. Ning, X. Li, C. Y. Lu, K. S. Novoselov, and A. A. Balandin, Nano Lett. **14**, 1497 (2014).
[11] T. Borca-Tasciuc, A. R. Kumar, and G. Chen, Rev. Sci. Instrum. **72**, 2139 (2001).
[12] T. Tong and A. Majumdar, Rev. Sci. Instrum. **77**, 104902 (2006).
[13] Z. Li, S. Tan, E. Bozorg-grayeli, T. Kodama, M. Asheghi, G. Delgado, M. Panzer, A. Pokrovsky, D. Wack, and K. E. Goodson, Nano Lett. **12**, 3121 (2012).
[14] J. Lee, Z. Li, J. P. Reifenberg, S. Lee, R. Sinclair, M. Asheghi, and K. E. Goodson, J. Appl. Phys. **109**, 084902 (2011).
[15] D. G. Cahill, Rev. Sci. Instrum. **61**, 802 (1990).
[16] K. Makoto, L. Yuxuan, J. Shenghong, M. Asuka, K. Shota, S. Takuma, K. Takashi, and S. Junichiro, ACS Appl. Energy Mater. **2**, 7083 (2019).
[17] J. S. Katz, W. Park, M. T. Barako, A. Sood, M. Asheghi, and K. E. Goodson, in *Solid-State, Actuators, Microsystems Workshop* (Transducer Research Foundation, 2018), pp. 280–283.
[18] J. S. Katz, M. T. Barako, W. Park, A. Sood, M. Asheghi, and K. E. Goodson, in *2018 17th IEEE Intersociety Conference on Thermal and Thermomechanical Phenomena in Electronic Systems* (IEEE, 2018), pp. 477–481.
[19] H. Ushirokita and H. Tada, Chem. Lett. **45**, 735 (2016).
[20] V. Linseis, F. Völklein, H. Reith, K. Nielsch, and P. Woias, Rev. Sci. Instrum. **89**, 015110 (2018).
[21] M. L. Bauer and P. M. Norris, Rev. Sci. Instrum. **85**, 064903 (2014).
[22] S. Roy-Panzer, T. Kodama, S. Lingamneni, M. A. Panzer, M. Asheghi, and K. E. Goodson, Rev. Sci. Instrum. **86**, 024901 (2015).
[23] S. D. Lubner, J. Choi, G. Wehmeyer, B. Waag, V. Mishra, H. Natesan, J. C. Bischof, and C. Dames, Rev. Sci. Instrum. **86**, 014905 (2015).
[24] M. T. Barako, A. Sood, C. Zhang, J. Wang, T. Kodama, M. Asheghi, X. Zheng, P. V. Braun, and K. E. Goodson, Nano Lett. **16**, 2754 (2016).
[25] M. T. Barako, S. Roy-Panzer, T. S. English, T. Kodama, M. Asheghi, T. W. Kenny, and K. E. Goodson, ACS Appl. Mater. Interfaces **7**, 19251 (2015).
[26] A. Feldman, High Temp. - High Pressures **31**, 293 (1999).
[27] M. E. DeCostera, K. E. Meyerb, B. D. Piercyc, J. T. Gaskinsa, B. F. Donovand, A. Giria, F. Nicholas, A. Strnade, D. M. Potrepkag, A. A. Wilsonh, M. D. Losegoc, and P. E. Hopkinsa, Thin Solid Films **650**, 71 (2018).
[28] K. Uetani, T. Okada, and H. T. Oyama, Biomacromolecules **16**, 2220 (2015).
[29] M. D. Losego, L. Moh, K. A. Arpin, D. G. Cahill, and P. V. Braun, Appl. Phys. Lett. **97**, 011908 (2010).
[30] M. Kosaka, J. Met. Finish. Soc. Jpn. **29**, 344 (1978).
[31] W. J. Parker, R. J. Jenkins, C. P. Butler, and G. L. Abbott, J. Appl. Phys. **32**, 1679 (1961).
[32] D. Zhao, X. Qian, X. Gu, S. A. Jajja, and R. Yang, J. Electron. Packag. **138**, 040802 (2016).
[33] C. Dames, S. Chen, C. T. Harris, J. Y. Huang, Z. F. Ren, M. S. Dresselhaus, and G. Chen, Rev. Sci. Instrum. **78**, 104903 (2007).
[34] M. Fujii, X. Zhang, H. Xie, H. Ago, K. Takahashi, T. Ikuta, H. Abe, and T. Shimizu, Phys. Rev. Lett. **95**, 065502 (2005).
[35] S. Yamaguchi, I. Tsunekawa, N. Komatsu, W. Gao, T. Shiga, T. Kodama, J. Kono, and J. Shiomi, Appl. Phys. Lett. **115**, 223104 (2019).
[36] G.-H. Kim, L. Shao, K. Zhang, and K. P. Pipe, Nat. Mater. **12**, 719 (2013).
[37] B. D. Washo and D. Hansen, J. Appl. Phys. **40**, 2423 (1969).
[38] X. T. Hao, T. Hosokai, N. Mitsuo, S. Kera, K. K. Okudaira, K. Mase, and N. Ueno, J. Phys. Chem. B **111**, 10365 (2007).
[39] X. Xie, D. Li, T.-H. Tsai, J. Liu, P. V. Braun, and D. G. Cahill, Macromolecules **49**, 972 (2016).
[40] X. Xie, K. Yang, D. Li, T. H. Tsai, J. Shin, P. V. Braun, and D. G. Cahill, Phys. Rev. B **95**, 035406 (2017).
[41] X. Wang, C. D. Liman, N. D. Treat, M. L. Chabinyc, and D. G. Cahill, Phys. Rev. B: Condens. Matter Mater. Phys. **88**, 075310 (2013).
[42] J. Liu, X. Wang, D. Li, N. E. Coates, R. A. Segalman, and D. G. Cahill, Macromolecules **48**, 585 (2015).
[43] Q. Wei, C. Uehara, M. Mukaida, K. Kirihara, and T. Ishida, AIP Adv. **6**, 045315 (2016).